

1 **Development of a Single-cycle Infectious SARS-CoV-2 Virus Replicon Particle System**
2 **for use in BSL2 Laboratories**

3

4 Johnny Malicoat^a, Senthamizharasi Manivasagam^a, Sonia Zuñiga^b, Isabel Sola^b, Dianne
5 McCabe^a, Lijun Rong^c, Stanley Perlman^a, Luis Enjuanes^b and Balaji Manicassamy^{a*}

6

7 ^a Department of Microbiology and Immunology, University of Iowa, Iowa City, IA, USA

8 ^b Coronavirus Laboratory, Departamento Biología Molecular y Celular, Centro Nacional de
9 Biotecnología (CNB-CSIC), Madrid, Spain

10 ^c Department of Microbiology and Immunology, University of Illinois at Chicago, IL, USA

11

12

13

14

15

16 *Address correspondence to Balaji Manicassamy

17 Email: balaji-manicassamy@uiowa.edu

18

19

20

21

22

23

24

25

26

27

28 Running title: Single-cycle Infectious SARS-CoV-2 Replicon

29

30

31

32

33 **Abstract**

34 Research activities with infectious severe acute respiratory syndrome associated coronavirus 2
35 (SARS-CoV-2) are currently permitted only under biosafety level 3 (BSL3) containment. Here,
36 we report the development of a single-cycle infectious SARS-CoV-2 virus replicon particle
37 (VRP) system with a luciferase and green fluorescent protein (GFP) dual reporter that can be
38 safely handled in BSL2 laboratories to study SARS-CoV-2 biology. The Spike (S) gene of
39 SARS-CoV-2 encodes for the envelope glycoprotein, which is essential for mediating infection
40 of new host cells. Through deletion and replacement of this essential S gene with a luciferase
41 and GFP dual reporter, we have generated a conditional SARS-CoV-2 mutant (Δ S-VRP) that
42 produces infectious particles only in cells expressing a viral envelope glycoprotein of choice.
43 Interestingly, we observed more efficient production of infectious particles in cells expressing
44 vesicular stomatitis virus (VSV) glycoprotein G (Δ S-VRP(G)) as compared to cells expressing
45 other viral glycoproteins including S. We confirmed that infection from Δ S-VRP(G) is limited to
46 a single round and can be neutralized by anti-VSV serum. In our studies with Δ S-VRP(G), we
47 observed robust expression of both luciferase and GFP reporters in various human and murine
48 cell types, demonstrating that a broad variety of cells can support intracellular replication of
49 SARS-CoV-2. In addition, treatment of Δ S-VRP(G) infected cells with anti-CoV drugs
50 remdesivir (nucleoside analog) or GC376 (CoV 3CL protease inhibitor) resulted in a robust
51 decrease in both luciferase and GFP expression in a drug-dose and cell-type dependent
52 manner. Taken together, we have developed a single-cycle infectious SARS-CoV-2 VRP
53 system that serves as a versatile platform to study SARS-CoV-2 intracellular biology and to
54 perform high throughput screening of antiviral drugs under BSL2 containment.

55
56
57
58
59
60
61
62
63

64 **Importance**

65 Due to the highly contagious nature of SARS-CoV-2 and the lack of immunity in the human
66 population, research on SARS-CoV-2 has been restricted to biosafety level 3 laboratories. This
67 has greatly limited participation of the broader scientific community in SARS-CoV-2 research
68 and thus has hindered the development of vaccines and antiviral drugs. By deleting the
69 essential Spike gene in the viral genome, we have developed a conditional mutant of SARS-
70 CoV-2 with luciferase and fluorescent reporters, which can be safely used under biosafety
71 level 2 conditions. Our single-cycle infectious SARS-CoV-2 virus replicon system can serve as
72 a versatile platform to study SARS-CoV-2 intracellular biology and to perform high throughput
73 screening of antiviral drugs under BSL2 containment.

74

75 **Introduction**

76 Due to the highly contagious nature of severe acute respiratory syndrome associated
77 coronavirus 2 (SARS-CoV-2) and the lack of sufficient immunity in the population, research on
78 SARS-CoV-2 is permitted only under BSL3 containment, which significantly limits SARS-CoV-
79 2 research only to institutions with BSL3 infrastructure. In addition, due to physical limitations,
80 high throughput screening of antiviral drugs can be impractical under BSL3 containment (1, 2).
81 Fortunately, research with attenuated or conditional mutants of BSL3/BSL4 pathogens is
82 allowed under lower containment upon demonstration of attenuation and safety (3). These
83 include low pathogenic H5N1 (lacking the multibasic site in HA), an Ebola virus conditional
84 mutant (VP30 deletion mutant), and *Yersinia pestis* conditional mutants, etc (4-6). Thus, to
85 enable studies with SARS-CoV-2 under BSL2 containment, SARS-CoV-2 spike (S)
86 pseudotyped HIV lentivirus particles or recombinant vesicular stomatitis virus (VSV) with the
87 native G gene replaced with the S gene have been developed and can be used to study the
88 viral entry process and to identify viral entry inhibitors (7-9). In addition, several SARS-CoV-2
89 replicon reporter systems that retain the minimal viral genes necessary for intracellular
90 replication have been developed (10-12). Moreover, conditional deletion mutants of SARS-
91 CoV-2 capable of replicating only in complemented cells expressing viral proteins have been
92 reported (N gene or ORF3a/E genes deleted) (13, 14). A recent study reported a single cycle
93 infectious particle system through co-expression of viral S, M, E and N proteins along with a
94 luciferase reporter carrying cis-acting elements (packaging sequences) of SARS-CoV-2 in the
95 3'UTR (15). The generation of these SARS-CoV-2 tools has allowed us to safely study various
96 aspects of SARS-CoV-2 biology under BSL2 containment.

97

98 Here, we report the development of a single-cycle infectious SARS-CoV-2 virus replicon
99 particle system (Δ S-VRP) with a luciferase and green fluorescent protein (GFP) reporter. Using
100 a bacterial artificial chromosome based reverse genetics system, we replaced the essential
101 spike gene of SARS-CoV-2 with a luciferase (Luc) and GFP dual reporter (Δ S-Luc-GFP) (16).
102 Co-transfection of the Δ S-Luc-GFP bacmid with a VSV-G expressing plasmid resulted in
103 efficient production of infectious VRPs (Δ S-VRP(G)), which can be further amplified in VSV-G
104 transfected cells. As expected, control vector transfected cells failed to produce any infectious
105 Δ S-VRPs, demonstrating that VRP infection is restricted to a single cycle. Δ S-VRP(G) stocks
106 produced from VSV-G expressing cells showed robust infection and expression of both

107 reporters in various murine and human cell lines, indicating that various cell types are
108 permissive to SARS-CoV-2 replication. Importantly, treatment of Δ S-VRP(G) infected cells with
109 antivirals Remdesivir (nucleoside analog) or GC376 (CoV 3CL protease inhibitor) resulted in a
110 robust and drug-dose dependent decrease in both luciferase and GFP reporter activity,
111 demonstrating that this platform can be useful for antiviral drug screening. Taken together, our
112 studies demonstrate that this Δ S-VRP system with a dual reporter can serve as a versatile tool
113 to investigate SARS-CoV-2 biology and perform antiviral drug screening under BSL2
114 containment.

115

116 **Results**

117 **Design of a single-cycle infectious SARS-CoV-2 virus replicon particle system**

118 To safely study SARS-CoV-2 biology under BSL2 containment, we deleted and replaced the
119 essential viral spike (S) ORF with a tandem Gaussia luciferase and Neon Green GFP dual
120 reporter separated by the porcine teschovirus 2A ribosome skipping signal under the control of
121 the S gene transcription regulatory sequence (Δ S-Luc-GFP; Fig 1A). Similar to other viral
122 replicons, the Δ S-Luc-GFP genome can undergo normal transcription and replication upon
123 transfection into cells, yet is unable to produce infectious virus particles due to the lack of the S
124 gene. As such, formation of infectious particles carrying the Δ S-Luc-GFP genome requires
125 expression of the S protein or other viral glycoprotein(s) in producer cells. We rescued
126 infectious VRPs by co-transfecting the Δ S-Luc-GFP bacmid with a VSV-G expression plasmid
127 into a mixture of 293T/Huh7.5 cells (Δ S-VRP(G); Fig 1B). We observed a significant increase
128 in luciferase activity in the supernatants and GFP expression in cells transfected with Δ S-Luc-
129 GFP bacmid over time as compared to control vector transfected cells (Fig 1C-D). On day 6
130 post-transfection, the 293T/Huh7.5 cell mixture was transfected again with a VSV-G
131 expression plasmid, which resulted in a significant increase in both luciferase activity and the
132 numbers of GFP expressing cells. These data show that Δ S-Luc-GFP replicated efficiently in
133 cells, and additional expression of VSV-G presumably increased the spread of Δ S-Luc-GFP
134 genome to new cells. To produce Δ S-VRP(G) working stocks, supernatants from Δ S-VRP(G)
135 rescue transfections were used as seed stocks to infect VSV-G expressing Huh7.5 cells. Next,
136 we evaluated the infectivity of amplified Δ S-VRP(G) stocks by measuring the expression of
137 viral nucleoprotein (N) and GFP in a human lung epithelial cell line (A549) expressing human
138 angiotensin-converting enzyme 2 (hACE2) (A549-hACE2). At 18hpi, immunofluorescence

139 analysis showed GFP expression in N positive cells (Fig 1E). Furthermore, western blot
140 analysis showed expression of N protein but not S protein in Δ S-VRP(G) infected cells (Fig
141 1F). Wild-type SARS-CoV-2 infected A549-hACE2 cell lysates were included as controls.
142 Taken together, we have successfully established a SARS-CoV-2 VRP system with a dual
143 reporter that can be easily propagated in VSV-G expressing cells.

144

145 **Δ S-VRP(G) infection is restricted to a single cycle and neutralized by anti-VSV sera**

146 Next, we compared the infectivity of Δ S-VRPs produced in Huh7.5 cells expressing
147 glycoproteins from diverse viral families including SARS-CoV-2 S and observed more efficient
148 production of infectious Δ S-VRPs only in cells expressing VSV-G (data not shown); hence, our
149 subsequent experiments were performed with Δ S-VRP(G) particles. Next, to demonstrate that
150 infection from Δ S-VRP(G) is restricted to a single round, we transferred the supernatants from
151 Δ S-VRP(G) infected Huh7.5 cells (No VSV-G transfection; R2 sup) onto fresh Huh7.5 cells and
152 observed no GFP or Luc expression. These results demonstrate that infection with Δ S-VRP(G)
153 is limited to a single cycle (Fig 2A).

154

155 Next, to assess the reproducibility of the Δ S-VRP(G) system, we tested the infectivity of 3
156 independent preparations of Δ S-VRP(G) stocks in Huh7.5 cells and observed similar levels of
157 luciferase activity across different preparations (Fig 2B). In addition, Δ S-VRP(G) preparations
158 were stable during storage at -80C and retained infectivity at levels similar to fresh Δ S-VRP(G)
159 preparations (Fig 2C). Moreover, we observed a dose dependent increase in the infectivity of
160 Δ S-VRP(G) in Huh7.5 cells. Next, to demonstrate that Δ S-VRP(G) infection is solely mediated
161 through the VSV-G glycoprotein, we tested if Δ S-VRP(G) infection can be inhibited in the
162 presence of anti-VSV serum (Fig 2D-E). Infectivity of Δ S-VRP(G) in Huh7.5 cells was
163 significantly reduced in the presence of anti-VSV serum as compared to control serum,
164 indicating that Δ S-VRP(G) infection is mediated through the VSV-G protein. Taken together,
165 we have developed a robust single-cycle infectious SARS-CoV-2 Δ S-VRP(G) dual reporter
166 system that can be safely used under BSL2 containment.

167

168 **Δ S-VRP(G) dual reporter system is a versatile tool to study SARS-CoV-2 biology in** 169 **different cell types**

170 As Δ S-VRP(G) infection of host cells is independent of SARS-CoV-2 host receptor ACE2
171 expression, we evaluated the robustness of the Δ S-VRP(G) dual reporter system in various
172 cell types of human and murine origin (Fig 3A-D). We observed robust replication of Δ S-Luc-
173 GFP in various cell types from different species including lung epithelial cells, kidney cells,
174 monocytic cell lines, lymphocytes, macrophages and dendritic cells. These results indicate that
175 several human and murine cell types are permissive to replication of SARS-CoV-2.
176 Interestingly, we observed differences in the levels of replication in different cells types,
177 indicating that cell specific host factors may regulate the intracellular replication steps of
178 SARS-CoV-2.

179

180 Next, to investigate if the Δ S-VRP(G) dual reporter system can be useful for the assessment of
181 host antiviral responses, we infected murine bone marrow derived macrophages (BMDM) and
182 dendritic cells (BMDC), and measured expression of the viral N gene and various host antiviral
183 genes. We observed robust induction of various antiviral genes including *Ifn α* , *Ifn β* , *Mx1*, *Isg15*
184 and *Tnf α* in BMDMs and to a lesser extent in BMDCs (Fig 3E). Taken together, these results
185 demonstrate that the Δ S-VRP(G) dual reporter system is a versatile tool to study SARS-CoV-2
186 biology as well as host immune responses in various cell types.

187

188 **Δ S-VRP(G) dual reporter system can be valuable for antiviral drug screening**

189 Next, to test if the Δ S-VRP(G) dual reporter system can be a useful platform for testing anti-
190 SARS-CoV-2 drugs, we assessed the effects of well-known anti-CoV drugs Remdesivir and
191 GC376 on Δ S-Luc-GFP replication (Fig 4). Huh7.5 or A549 cells infected with Δ S-VRP(G) were
192 treated with different concentrations of Remdesivir or GC376 starting at 2hpi. At 18hpi, both
193 luciferase activity in the supernatants and GFP expression in infected cells were compared
194 between different treatment groups. In Huh7.5 cells, we observed a dose dependent decrease
195 in luciferase activity along with a concomitant decrease in GFP expression in both Remdesivir
196 and GC376 treatment groups as compared to DMSO treated cells (Fig 4A and 4C; Remdesivir
197 IC₅₀ 26.7nM and GC376 IC₅₀ 17.3nM). We also observed a similar dose dependent inhibition
198 of Δ S-Luc-GFP replication in A549 cells treated with either Remdesivir or GC376 (Fig 4B and
199 4D; Remdesivir 55.2nM and GC376 2300 nM); Interestingly, inhibition of Δ S Luc-GFP
200 replication by Remdesivir and GC376 was less pronounced in A549 cells as compared to
201 Huh7.5 cells, indicating cell type specific differences in the activity of antiviral drugs. These

202 results demonstrate that the Δ S-VRP(G) dual reporter system can be useful for rapid screening
203 of antiviral drugs against SARS-CoV-2 under BSL2 containment. Taken together, we have
204 successfully established a SARS-CoV-2 VRP dual reporter platform that allows for safe
205 investigation of SARS-CoV-2 biology, host interactions, and antiviral responses, as well as for
206 high throughput screening of anti-CoV drugs, under BSL2 containment.

207

208 **Discussion**

209 Studies with highly pathogenic viruses can be safely performed in biological laboratories with
210 specialized biocontainment procedures. Through the generation of conditional replicating
211 mutants or attenuated mutants, we can safely study some aspects of virus biology in standard
212 BSL2 or BSL2+ facilities. Currently, research activities with SARS-CoV-2 are restricted to
213 BSL3 facilities that mostly have limited capabilities. To overcome this limitation, we have
214 developed a conditional mutant of SARS-CoV-2 through deletion and replacement of the
215 essential viral S glycoprotein gene with a luciferase-GFP dual reporter, leaving the remaining
216 SARS-CoV-2 genome intact. Through co-expression of VSV-G protein *in trans*, we have
217 successfully generated single-cycle infectious SARS-CoV-2 replicon particles carrying the Δ S
218 Luc-GFP genome. Various human and murine cells infected with Δ S-VRP(G) showed robust
219 expression of both luciferase and GFP reporters, indicating that these cell lines are permissive
220 to intracellular replication of SARS-CoV-2. In addition, as viral entry of Δ S-VRP(G) particles is
221 mediated through the G protein, Δ S-VRP(G) can efficiently infect a variety of human and
222 murine cell types lacking the SARS-CoV-2 ACE2 receptor. Importantly, the Δ S-VRP(G) dual
223 reporter system showed robust responsiveness to treatment with Remdesivir or GC376,
224 demonstrating that the Δ S-VRP(G) dual reporter system can be useful for high-through put
225 screening of antiviral drugs against SARS-CoV-2.

226

227 Several groups have reported the development of SARS-CoV-2 replicon systems with either
228 luciferase or GFP reporters, and the majority of these replicon systems require transfection of
229 replicon DNA or RNA into cells, which may limit studies to cell types with higher transfection
230 efficiency. In addition, there might be a time lag between nucleic acid transfection and optimal
231 reporter expression. One advantage of our Δ S-VRP(G) dual reporter system is that large
232 quantities of Δ S-VRP(G) can be easily amplified in VSV-G expressing Huh7.5 cells, and can
233 be used to investigate SARS-CoV-2 biology in a variety of cell types. In addition to replicons,

234 conditional SARS-CoV-2 mutants with GFP or luciferase reporters have been developed. Ju,
235 et al. generated a mutant lacking a portion of the essential N gene, thereby limiting replication
236 to cells expressing N (14). Zhang, et al. generated a conditional mutant lacking the ORF3a/E
237 genes, which restricted replication to cells stably expressing ORF3a and E proteins (13). As an
238 additional safety measure, these authors elegantly modified all TRS sites to restrict the
239 potential emergence of replication competent virus through recombination with wild-type
240 SARS-CoV-2. Another advantage of our Δ S-VRP(G) system is that VSV-G mediated delivery
241 of the Δ S-Luc-GFP genome occurs independently of the ACE2 receptor. Indeed, a vast
242 majority of human and murine cell types supported Δ S-Luc-GFP replication, albeit with some
243 differences in the levels of replication. It is possible that the observed variations in Δ S-Luc-GFP
244 replication can be in part due to inherent differences in VSV-G mediated entry into various cell
245 types. Finally, as the Δ S-VRP(G) system contains both luciferase and GFP reporters, we
246 observed a strong co-relation between luciferase activity and GFP expression across different
247 treatment groups in our studies with remdesivir and GC376. The presence of a dual reporter
248 allows for rapid elimination of false positive hits that directly inhibit luciferase or interfere with
249 GFP fluorescence during high-throughput antiviral drug screening.

250

251 In our studies, we observed robust luciferase and GFP expression in cells infected with Δ S-
252 VRP(G) as compared to Δ S-VRP produced in cells expressing other viral glycoproteins
253 including SARS-CoV-2 S (data not shown). We speculate that this is in part due to the higher
254 efficiency of VSV-G protein in mediating viral entry as compared to other viral glycoproteins. It
255 is not completely clear how VSV-G is incorporated onto Δ S-VRPs to mediate infection. VSV-G
256 has been reported to be localized to intracellular compartments, such as the endoplasmic
257 reticulum-golgi, as well as on the plasma membrane. As SARS-CoV-2 assembly and budding
258 is thought to occur in the endoplasmic reticulum-golgi intermediate compartment (ERGIC), it is
259 possible that intracellularly expressed VSV-G is incorporated onto VRP membranes during
260 canonical SARS-CoV-2 budding in the ERGIC. In agreement with VSV-G dependent delivery
261 of the Δ S Luc-GFP genome, Δ S-VRP(G) infection was neutralized in the presence of anti-VSV
262 sera. Our future studies will determine if VSV-G incorporation onto Δ S-VRPs occurs in
263 intracellular compartments.

264

265 In conclusion, we have developed a SARS-CoV-2 VRP platform with a dual reporter that can
266 serve as a versatile tool to study SARS-CoV-2 host biology under BSL2 containment.
267 Importantly, we observed robust and dose dependent changes in both luciferase and GFP
268 expression upon treatment with anti-CoV drugs, demonstrating that this Δ S-VRP(G) platform
269 can be suitable for safe high throughput screening of antivirals against SARS-CoV-2.
270

271 **Materials and Methods**

272 **Biosafety statement**

273 Studies with infectious SARS-CoV-2 and Δ S-VRP(G) viruses were approved by Ulowa IBC
274 and CCOM BSL3 Oversight Committee (Protocol # 210053). Initial validation and safety
275 studies with Δ S-VRP(G) were performed in a BSL3 laboratory. After review of the safety data,
276 both Ulowa IBC and the NIH Office of Science Policy approved the use of Δ S-VRP(G) under
277 BSL2+ containment at Ulowa.
278

279 **Ethics statement**

280 All studies were performed in accordance with the principles described by the Animal Welfare
281 Act and the National Institutes of Health guidelines for the care and use of laboratory animals
282 in biomedical research. The protocol for isolating anti-VSV serum from mice was reviewed and
283 approved by the Institutional Animal Care and Use Committee at the University of Iowa
284 (Animal Protocol #1062127).
285

286 **Anti-VSV serum**

287 Antisera against VSV was produced in-house by immunizing C57BL/6J mice (6 weeks old)
288 with 2×10^8 PFU of live VSV-GFP virus via intramuscular route. On day 14, mice were boosted
289 with the same dose of VSV-GFP virus. At 4 weeks post-immunization, serum was collected by
290 cardiac puncture and used in neutralization experiments after heat inactivation.
291

292 **Cell lines and primary cells**

293 Human lung epithelial cells (A549), human embryonic kidney cells (HEK293T), hepatocellular
294 carcinoma cell line (Huh7.5), mouse endothelial cell line (MS1), mouse lung epithelial cells
295 (LA4), mouse macrophage cell line (Raw 264.7), and African green monkey kidney epithelial
296 cells (Vero) were cultured in Dulbecco's Modified Eagle Medium (DMEM) supplemented with
297 10% fetal bovine serum (FBS) and 1% penicillin/streptomycin (10,000U/ml). Primary bone

298 marrow derived macrophages (BMDM) and dendritic cells (BMDC) were generated from bone
299 marrows isolated from C57BL/6J mice (Jackson labs) by culturing in the presence of IL-4 and
300 GM-CSF or IL-4 and L929 conditioned media, respectively (17, 18).

301

302 **Generation of Δ S-Luc-GFP bacmid**

303 SARS-CoV-2 reverse genetics system based on the sequence of Wuhan-Hu-1/2019 isolate
304 (Accession number: NC_045512) was designed and assembled into a pBeloBac11 vector as
305 previously described for other coronaviruses (16). Our SARS-CoV-2 bacmid carries a unique
306 engineered SanDI restriction site in the NSP15 gene and a naturally occurring unique BamHI
307 restriction site near the 3' end of the S gene (70 nucleotides before ORF3a TRS). A gene
308 fragment representing the dual reporter under S TRS was chemically synthesized as a 1.7kb
309 gBlock fragment (Integrated DNA Technologies) in the following in-frame arrangement of
310 reporters: S gene TRS, S signal peptide (MFVFLVLLPLVSSQC), Gaussia luciferase, porcine
311 teschovirus 2A site (ATNFSLLKQAGDVEENPG↓P), and Neon Green GFP reporter. The
312 genomic sequence between the SanDI site and the S TRS was PCR amplified using PrimeStar
313 Max (Clontech). Both fragments were combined together by fusion PCR and subsequently
314 cloned into the SARS-CoV-2 bacmid cut with SanDI and BamHI enzymes using the HiFi
315 assembly system (NEB). Assembly mixtures were transformed into DH10Bac and individual
316 Δ S-Luc-GFP bacmid clones were identified by restriction digestion of bacmid DNA.

317

318 **Rescue and amplification of Δ S-VRP(G)**

319 To rescue recombinant Δ S-VRP(G) virus, a mixture of 293T cells/Huh7.5 cells in suspension
320 (1×10^6 cells each cell type) were transfected with $4 \mu\text{g}$ of Δ S-Luc-GFP bacmid and $1 \mu\text{g}$ of VSV-
321 G plasmid (Addgene #138479) using PEI transfection reagent (Polysciences; DNA:PEI ratio
322 1:4). After 5hrs post-transfection, the transfection mixture containing media was replaced with
323 DMEM/2%FBS media. At 72-96hrs post-transfection, supernatants were collected and kept as
324 Δ S-VRP(G) seed stocks. To amplify Δ S-VRP(G), Huh7.5 cells seeded in 150mm plates
325 (1.5×10^7) were transfected with $40 \mu\text{g}$ of VSV-G plasmid using PEI reagent. At 5hrs post-
326 transfection, the transfection mixture containing media was replaced with DMEM/10% FBS
327 media. On the following day, 1ml of Δ S-VRP(G) seed stock was added to VSV-G transfected
328 Huh7.5 cells and incubated for 2hrs. After washing with PBS, infected Huh7.5 cells were
329 placed in 25ml of DMEM/2% FBS, and monitored for GFP expression and cytopathic effects

330 (CPE). At 48-72h post infection, supernatants were collected, clarified of debris, aliquoted and
331 stored at -80C. These stocks were used to perform subsequent infection experiments.

332

333 **ΔS-VRP(G) infection**

334 Indicated cell types were seeded in 12-well ($1-2 \times 10^5$ per well) or 6-well plates ($5-8 \times 10^5$ per
335 well) a day prior to infection and infected with 0.5ml or 1ml of ΔS-VRP(G) stock, respectively.

336 After 2hr incubation, viral inoculum was removed and replaced with DMEM/2%FBS media,
337 after two PBS washes. At 18hpi, luciferase activity in the supernatant and GFP expression in
338 the cells were measured. For measurement of luciferase activity, 50ul of supernatant was
339 mixed with 50ul of Renilla luciferase substrate (Promega) and immediately measured in a
340 GloMax 20/20 single tube luminometer. GFP images were captured with a Nikon Eclipse
341 microscope using a 20X objective at an exposure time of 600 mSec.

342

343 **Remdesivir and GC376 inhibition**

344 A549 or Huh7.5 cells seeded at a density of 1.5×10^5 per well (12-well plate) a day prior were
345 infected with 0.5ml of ΔS-VRP(G) stock. After 2hpi, cells were washed with PBS and placed in
346 DMEM/2%FBS media with the indicated amounts of drug. Measurement of luciferase activity
347 and GFP expression were performed as described above at 18hpi.

348

349 **Immunofluorescence**

350 A day prior to infection, A549 cells were seeded onto glass coverslips at 1×10^5 cells/well in a
351 24-well plate in Opti-Modified Eagle Medium (Opti-MEM) and infected with 0.5ml of ΔS-
352 VRP(G). After 2hrs, viral inoculum was replaced with Opti-MEM. At 18hpi, infected cells were
353 washed twice with PBS and fixed with 4% Paraformaldehyde (Electron Microscopy Sciences)
354 in PBS for 5 min at room temperature. After washing with PBS, fixed cell were permeabilized
355 with 0.3% Triton X-100 in PBS for 5 min, washed with PBS and incubated in a blocking buffer
356 consisting of 1% BSA, 0.5% fish gelatin (Sigma), and 0.01% Tween20 (Sigma) in PBS for 30
357 min. Permeabilized cells were incubated in blocking buffer with mouse anti-nucleoprotein
358 antibody (1:1000 from Sino Biological) for 1hr followed by staining with goat anti-mouse
359 Alexa647 secondary antibody for 30min. Coverslips were mounted onto microscopy slides with
360 ProLong Gold Antifade Mountant with DAPI (Invitrogen). All incubations involving antibody
361 staining were performed with gentle shaking at room temperature. Images were acquired on a

362 Leica DFC7000T microscope under 63x oil-immersion objective using Leica software and
363 processed using ImageJ software.

364 **Western blot analysis**

365 A549 cells seeded in 6-well plates at 1×10^6 cells/well were infected with 1ml of Δ S-VRP(G) and
366 at 18hpi, cells were lysed in RIPA buffer and protein samples were separated on a 4-15%
367 gradient SDS-PAGE gel (Bio-Rad). As controls, A549-hACE2 cells were infected with SARS-
368 COV-2 (Wuhan-Hu-1/2019) at an MOI of 3 and lysed in RIPA buffer. Western blot analysis was
369 performed following the transfer of proteins onto a nitrocellulose membrane using mouse anti-
370 nucleoprotein or S antibody (1:1000 from Sino Biological) and goat α -mouse secondary
371 antibody conjugated to horseradish peroxidase (#GENA931, Sigma).

372 **Quantitative RT-PCR analysis**

373 BMDM and BMDC seeded at a density of 2×10^6 cells/well were infected with 2ml of Δ S-
374 VRP(G) and at 18hpi, total RNA from infected cells were extracted using PureLink RNA
375 extraction kit according to manufacturer's instructions. Residual genomic DNA contamination
376 was removed by DNase I (Invitrogen Cat #12185010) treatment. cDNA was synthesized using
377 Superscript IV Reverse Transcriptase (Invitrogen Cat #18090010) and Oligo d(T) (Invitrogen)
378 and qPCR analysis was performed using SYBR Green PCR Master Mix (Applied Biosystem
379 Cat #4368702) with technical duplicates and gene specific primers (19). 18S RNA was used as
380 an endogenous house housekeeping gene to calculate delta delta cycle thresholds. qPCR
381 primers are as follows - SARS-CoV-2 N forward: CAATGCTGCAATCGTGCTAC and reverse
382 GTTGCGACTACGTGATGAGG; mouse *Iln* α 1 forward: TCAAAGGACTCATCTGCTGCTTG
383 and reverse CCACCTGCTGCATCAGACAAC; mouse *Iln* β forward:
384 CAGTCCAAGAAAGGACGAAC and reverse: GGCAGTGTA ACTCTTCTGCAT; Mx1 forward:
385 GACCATAGGGGTCTTGACCAA and reverse: AGACTTGCTCTTTCTGAAAAGCC; *Isg15*
386 forward: GGTGTCCGTGACTAACTCCAT and reverse: TGGAAAGGGTAAGACCGTCCT; *Tnfa*
387 forward: GACGTGGA ACTGGCAGAAGAG and reverse: TTGGTGGTTTGTGAGTGTGAG;
388 18S forward: AAACGGCTACCACATCCAAG and reverse: CCTCCAATGGATCCTCGTTA.
389 Results are represented as fold expression relative to mock samples.

390

391 **Statistical analysis**

392 Significance of data points was assessed using the unpaired Student's t-test. * denotes p-
393 value <0.05 and ns denotes non-significant.

394

395 **Acknowledgements**

396 We would like to thank Drs. Lok-Yin Roy Wong and Ruangang Pan from the Perlman lab and
397 Dr. Thomas Gallagher for their advice on coronavirus bacmid system.

398

399

400

401

402

403

404

405

406

407

408

409

410

411

412

413

414

415

416

417

418

419

420

421

422

423 **Figure Legends**

424 **Fig 1. Development of single-cycle infectious SARS-CoV-2 replicon system with a dual**
425 **reporter.** (A) Schematic representation of SARS-CoV-2 and Δ S Luc-GFP SARS-CoV-2
426 genomes. The S gene in the SARS-CoV-2 genome was replaced with a luciferase and GFP
427 dual reporter. (B) Generation and amplification of Δ S virus replicon particles. Left:
428 293T/Huh7.5 cell mixture was transfected with Δ S Luc-GFP bacmid and VSV-G plasmid.
429 Right: Supernatants from Δ S-VRP(G) rescue transfections were amplified in Huh7.5 cells
430 transfected with VSV-G plasmid. (C-D) Kinetics of luciferase and GFP expression during
431 rescue transfection process. 293T/Huh7.5 cells were co-transfected with Δ S Luc-GFP bacmid
432 and VSV-G plasmid, and at various days post-transfection, luciferase activity in the
433 supernatants and GFP expression in the cell mixture were assessed. On day 6 post-
434 transfection, 293T/Huh7.5 cells were again transfected with additional VSV-G plasmid. (C)
435 Luciferase values and (D) GFP expression are shown at the indicated time points. Luciferase
436 activity is shown for 3 independent Bac clones. GFP expression is shown for Bac clone #7. (E)
437 Immunofluorescence imaging of GFP and nucleoprotein expression in Δ S-VRP(G) infected
438 cells. A549-hACE2 cells were infected with Δ S-VRP(G) and at 18hpi, cells were stained with
439 anti-N antibody and imaged. (F) Western blot analysis of nucleoprotein expression in Δ S-
440 VRP(G) infected cells. A549-hACE2 cells were infected with Δ S-VRP(G) and at 18hpi, cell
441 lysates were collected and analyzed for nucleoprotein and spike protein expression by western
442 blot. Cell lysates from wild type SARS-CoV-2 infected cells were included as controls. β -actin
443 levels are shown as loading controls.

444
445
446 **Fig 2. Characterization of Δ S-VRP dual reporter system.** (A) Δ S-VRP(G) infection is
447 restricted to a single round. Huh7.5 cells were infected with Δ S-VRP(G) and at 2hpi, cells were
448 washed and incubated in fresh media. At 48h, supernatants (Round 2 - R2 sup) were collected
449 and added to new Huh7.5 cells. At 18hpi, luciferase activity in the supernatant was measured.
450 (B) Comparison of infectivity of different Δ S-VRP(G) preparations. Huh7.5 cells were infected
451 with 3 independent preparations of Δ S-VRP(G) and luciferase activity was measured at 18hpi.
452 (C) Infectivity of Δ S-VRP(G) stored at -80C. Huh7.5 cells were infected with Δ S-VRP(G) stored
453 at -80C or fresh preparations and luciferase activity was measured at 18hpi. (D-E)
454 Neutralization of Δ S-VRP(G) infection by anti-VSV sera. Sera from Control (Cntrl) and VSV-
455 infected mice were pre-incubated with Δ S-VRP(G) for 1 hour and subsequently incubated with

456 Huh7.5 cells for 2 hours. Luciferase and GFP expression were assessed at 18hpi. For panels
457 B-E, luciferase activity in the supernatants was measured and is shown as relative light units
458 (RLU). For panel G, luciferase activity was normalized to No Treatment control and is shown
459 as percentage (%) of No Treatment control.

460

461 **Fig 3. Permissiveness of human and murine cells to Δ S Luc-GFP replication.** The
462 indicated human and murine cells were infected with Δ S-VRP(G) and at 18hpi, luciferase
463 activity and GFP expression were measured. (A-B) Luciferase expression in human and
464 murine cell lines. (C-D) GFP expression in human and murine cell lines. (E-F) Primary BMDM
465 and BMDC were infected with Δ S-VRP(G) and at 18hpi, expression of viral N mRNA and host
466 antiviral genes were measured by qRT-PCR. (E) Viral N mRNA expression and (F) host
467 antiviral gene expression.

468

469

470 **Fig 4. Δ S-VRP(G) reporter system is suitable for antiviral drug screening.** Huh7.5 or
471 A549 cells were infected with Δ S-VRP(G) virus and at 2hpi, infected cells were treated with the
472 indicated concentrations of Remdesivir or GC376 dissolved in DMSO. At 18hpi, GFP
473 expression and luciferase activity were measured. (A-B) Assessment of effects of Remdesivir
474 treatment on Δ S Luc-GFP replication in Huh7.5 and A549 cells. (C & D) Assessment of effects
475 of GC376 treatment on Δ S Luc-GFP replication in Huh7.5 and A549 cells. Luciferase values
476 are normalized to DMSO control and shown as % DMSO control.

477

478

479

480

481

482

483

484

485

486

487

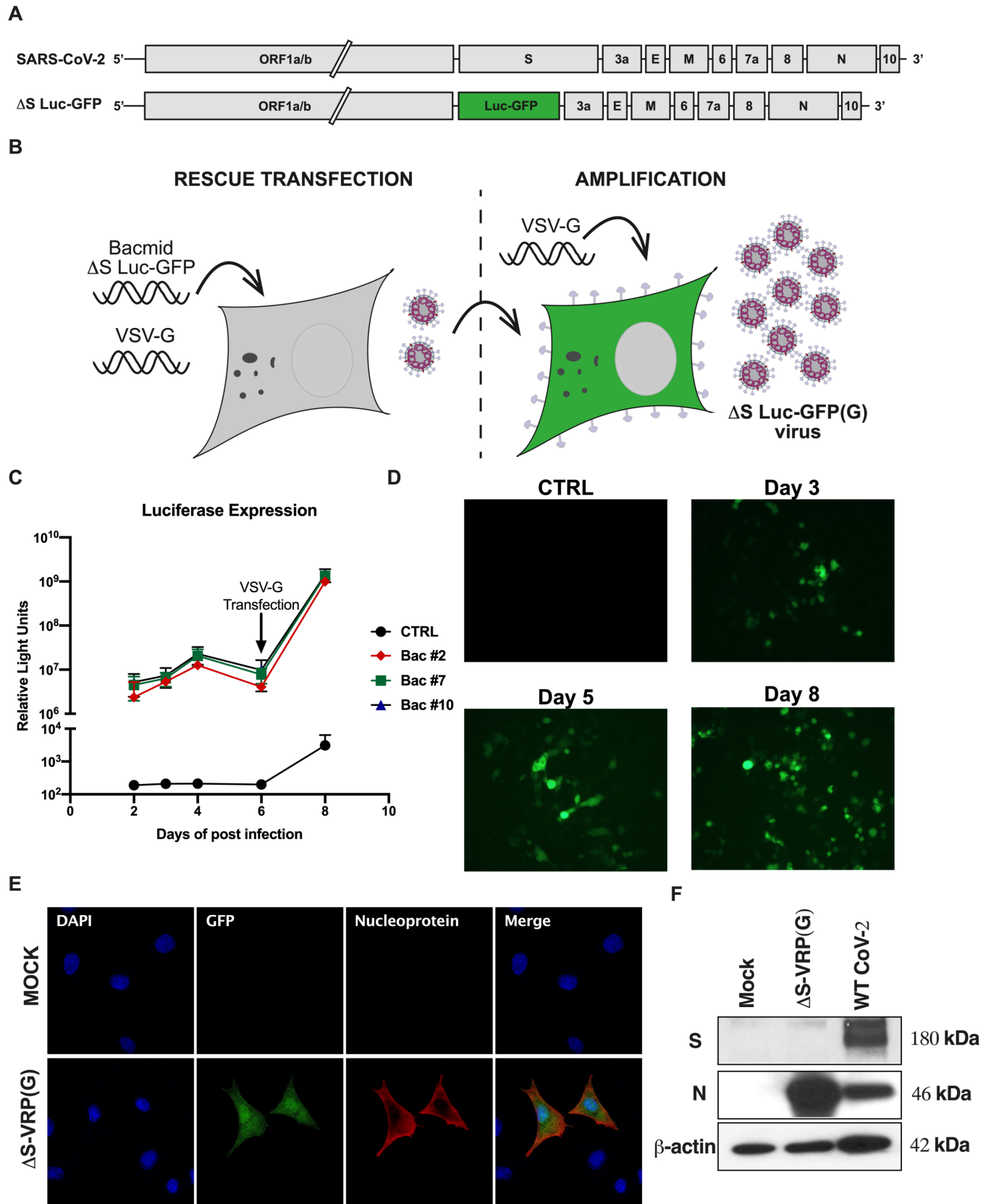
488

489 **References**

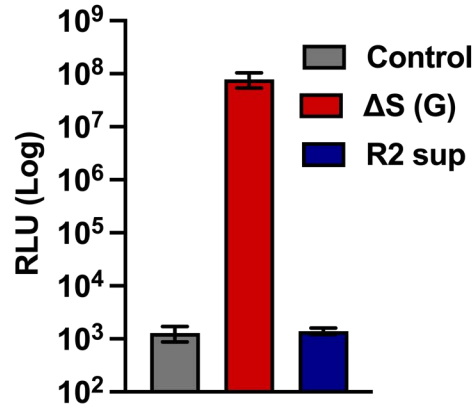
490

- 491 1. Friedrich B, Scully C, Brannan J. 2011. Assessment of High-Throughput Screening
492 (HTS) Methods for High-Consequence Pathogens. *Journal of Bioterrorism & Biodefense*
493 02.
- 494 2. Rasmussen L, Tigabu B, White EL, Bostwick R, Tower N, Bukreyev A, Rockx B, LeDuc
495 JW, Noah JW. 2015. Adapting high-throughput screening methods and assays for
496 biocontainment laboratories. *Assay Drug Dev Technol* 13:44-54.
- 497 3. Anonymous. Select Agents and Toxins Exclusions: Excluded Attenuated Strains of HHS
498 Select Agents, Section 73.3 (e).
- 499 4. Kuroda M, Halfmann PJ, Hill-Batorski L, Ozawa M, Lopes TJS, Neumann G, Schoggins
500 JW, Rice CM, Kawaoka Y. 2020. Identification of interferon-stimulated genes that
501 attenuate Ebola virus infection. *Nat Commun* 11:2953.
- 502 5. Centers for Disease C, Prevention, Gangadharan D, Smith J, Weyant R. 2013.
503 Biosafety Recommendations for Work with Influenza Viruses Containing a
504 Hemagglutinin from the A/goose/Guangdong/1/96 Lineage. *MMWR Recomm Rep* 62:1-
505 7.
- 506 6. Galvan EM, Nair MK, Chen H, Del Piero F, Schifferli DM. 2010. Biosafety level 2 model
507 of pneumonic plague and protection studies with F1 and Psa. *Infect Immun* 78:3443-53.
- 508 7. Crawford KHD, Eguia R, Dingens AS, Loes AN, Malone KD, Wolf CR, Chu HY, Tortorici
509 MA, Veesler D, Murphy M, Pettie D, King NP, Balazs AB, Bloom JD. 2020. Protocol and
510 Reagents for Pseudotyping Lentiviral Particles with SARS-CoV-2 Spike Protein for
511 Neutralization Assays. *Viruses* 12.
- 512 8. Dieterle ME, Haslwanter D, Bortz RH, 3rd, Wirchnianski AS, Lasso G, Vergnolle O,
513 Abbasi SA, Fels JM, Laudermilch E, Florez C, Mengotto A, Kimmel D, Malonis RJ,
514 Georgiev G, Quiroz J, Barnhill J, Pirofski LA, Daily JP, Dye JM, Lai JR, Herbert AS,
515 Chandran K, Jangra RK. 2020. A Replication-Competent Vesicular Stomatitis Virus for
516 Studies of SARS-CoV-2 Spike-Mediated Cell Entry and Its Inhibition. *Cell Host Microbe*
517 28:486-496 e6.
- 518 9. Case JB, Rothlauf PW, Chen RE, Liu Z, Zhao H, Kim AS, Bloyet LM, Zeng Q, Tahan S,
519 Droit L, Ilagan MXG, Tartell MA, Amarasinghe G, Henderson JP, Miersch S, Ustav M,
520 Sidhu S, Virgin HW, Wang D, Ding S, Corti D, Theel ES, Fremont DH, Diamond MS,
521 Whelan SPJ. 2020. Neutralizing Antibody and Soluble ACE2 Inhibition of a Replication-
522 Competent VSV-SARS-CoV-2 and a Clinical Isolate of SARS-CoV-2. *Cell Host Microbe*
523 28:475-485 e5.
- 524 10. Nguyen HT, Falzarano D, Gerdtz V, Liu Q. 2021. Construction of a non-infectious
525 SARS-CoV-2 replicon for antiviral drug testing and gene function studies. *J Virol*
526 doi:10.1128/JVI.00687-21:JVI0068721.
- 527 11. He X, Quan S, Xu M, Rodriguez S, Goh SL, Wei J, Fridman A, Koeplinger KA, Carroll
528 SS, Grobler JA, Espeseth AS, Olsen DB, Hazuda DJ, Wang D. 2021. Generation of
529 SARS-CoV-2 reporter replicon for high-throughput antiviral screening and testing. *Proc*
530 *Natl Acad Sci U S A* 118.
- 531 12. Luo Y, Yu F, Zhou M, Liu Y, Xia B, Zhang X, Liu J, Zhang J, Du Y, Li R, Wu L, Zhang X,
532 Pan T, Guo D, Peng T, Zhang H. 2021. Engineering a Reliable and Convenient SARS-
533 CoV-2 Replicon System for Analysis of Viral RNA Synthesis and Screening of Antiviral
534 Inhibitors. *mBio* 12.
- 535 13. Zhang X, Liu Y, Liu J, Bailey AL, Plante KS, Plante JA, Zou J, Xia H, Bopp NE, Aguilar
536 PV, Ren P, Menachery VD, Diamond MS, Weaver SC, Xie X, Shi PY. 2021. A trans-

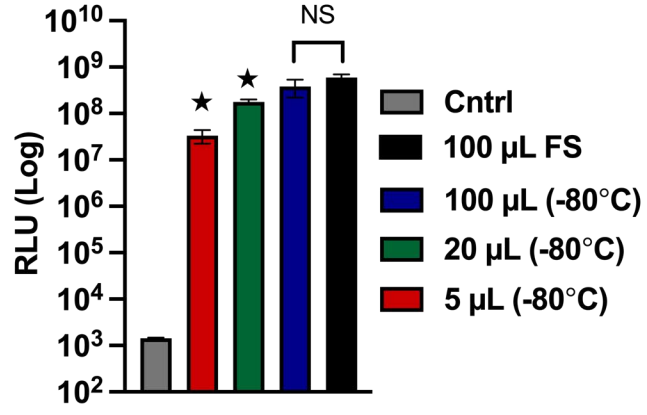
- 537 complementation system for SARS-CoV-2 recapitulates authentic viral replication
538 without virulence. *Cell* 184:2229-2238 e13.
- 539 14. Ju X, Zhu Y, Wang Y, Li J, Zhang J, Gong M, Ren W, Li S, Zhong J, Zhang L, Zhang
540 QC, Zhang R, Ding Q. 2021. A novel cell culture system modeling the SARS-CoV-2 life
541 cycle. *PLoS Pathog* 17:e1009439.
- 542 15. Syed AM, Taha TY, Tabata T, Chen IP, Ciling A, Khalid MM, Sreekumar B, Chen PY,
543 Hayashi JM, Soczek KM, Ott M, Doudna JA. 2021. Rapid assessment of SARS-CoV-2
544 evolved variants using virus-like particles. *Science*
545 doi:10.1126/science.abl6184:eabl6184.
- 546 16. Almazan F, Marquez-Jurado S, Nogales A, Enjuanes L. 2015. Engineering infectious
547 cDNAs of coronavirus as bacterial artificial chromosomes. *Methods Mol Biol* 1282:135-
548 52.
- 549 17. Kandasamy M, Suryawanshi A, Tundup S, Perez JT, Schmolke M, Manicassamy S,
550 Manicassamy B. 2016. RIG-I Signaling Is Critical for Efficient Polyfunctional T Cell
551 Responses during Influenza Virus Infection. *PLoS pathogens* 12:e1005754.
- 552 18. Schmolke M, Manicassamy B, Pena L, Sutton T, Hai R, Varga ZT, Hale BG, Steel J,
553 Perez DR, Garcia-Sastre A. 2011. Differential contribution of PB1-F2 to the virulence of
554 highly pathogenic H5N1 influenza A virus in mammalian and avian species. *PLoS*
555 *pathogens* 7:e1002186.
- 556 19. Han J, Perez JT, Chen C, Li Y, Benitez A, Kandasamy M, Lee Y, Andrade J, tenOever
557 B, Manicassamy B. 2018. Genome-wide CRISPR/Cas9 Screen Identifies Host Factors
558 Essential for Influenza Virus Replication. *Cell Rep* 23:596-607.
- 559



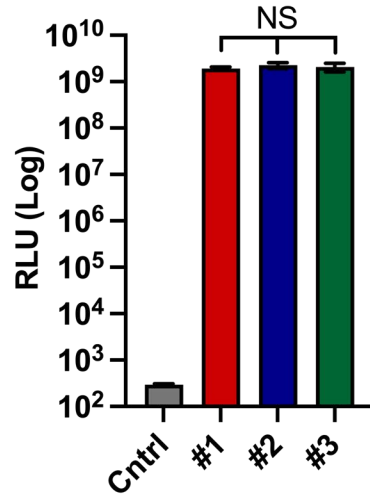
A



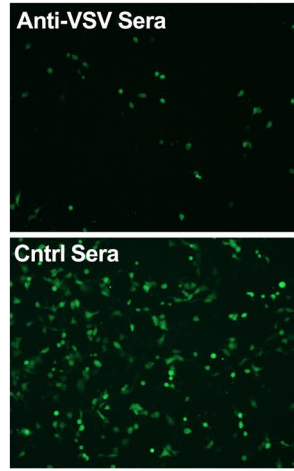
C



B



D



E

